BELLE2-NOTE-PL-2020-015
July 28, 2020

L1 trigger efficiencies for $e^+e^- \to \tau^+\tau^-$ events

The Belle II Collaboration

Abstract

The Level 1 trigger efficiency has been studied in τ-pair events. The $ee \to \tau\tau \to 1{\times}3$ prong and $1{\times}1$ prong decay signatures are considered. These measurements were performed using the e^+e^- collision data recorded during the 2019a, 2019b and 2019c data taking periods. This document contains the approved plots and captions.

In this note we present the measurement of the Level 1 (L1) trigger efficiency for $e^+e^- \to \tau^+\tau^-$ events in 2019 data (periods 2019a, 2019b and 2019c). This data sample corresponds to a total integrated luminosity of 8.8 fb^{-1}.

The cross section for the process $e^+e^- \to \tau^+\tau^-$ is of the same order as the production of B meson pairs at the $\Upsilon(4S)$ resonance energy. In addition, τ lepton decays result in a wide variety of low multiplicity signatures involving tracks ($e^\pm$, $\mu^\pm$ or $\pi^\pm$) and ECL clusters ($e^\pm$, $\mu^\pm$, $\pi^\pm$ or π^0). Considering this, τ-pair events provide a good test bed for the performance of both the CDC and ECL triggers.

Three τ-pair decay modes are considered:

- *SM 1×1* — both τ leptons undergo Standard Model (SM) decay into one charged particle (1-prong). This can occur via the leptonic decay mode ($\tau^\pm \to \ell^\pm \nu_\ell \bar{\nu_\tau}$, $\ell = e, \mu$) or hadronic mode with one charged pion ($\tau^\pm \to \pi^\pm \nu_\tau + n\pi^0$).
- *SM 1×3* — one τ lepton undergoes SM 1-prong decay while the other undergoes SM decay into three charged pions (3-prong). The latter occurs through the hadronic decay mode with three charged pions ($\tau^\pm \to 3\pi^\pm \nu_\tau + n\pi^0$).
- *LFV 1×3* — one τ lepton decays undergoes SM 1-prong decay while the other undergoes Lepton Flavour Violating (LFV) decay into three muons. This targets one of the golden channels for LFV searches in τ decays at *Belle II* ($\tau \to 3\mu$). The strategy is to select SM 1×3 prong events that mimic the kinematics of the LFV process.

Six channels are considered according to whether the tracks are identified as electrons, muons or charged pions. For 1×1 prong decay we consider the $e\mu$, $\mu\pi$ and $\mu\mu$ channels. For 1×3 prong decay we have the $e - 3\pi$, $\mu - 3\pi$ and $\pi - 3\pi$ channels.

The following triggers have been studied:

- *CDC full tracks* — ffo and fff.
- *CDC short tracks* — fso, sso, ffs, fss and sss.
- *ECL* — hie, c4 and eclmumu.
- *ECL low multiplicity* — lml0, lml1, lml2, lml4, lml6, lml7, lml8, lml9, lml10 and lml12.

We define the efficiency of an individual CDC trigger as:

$$\epsilon = \frac{\text{(hie or c4 or eclmumu or lmlX) and CDC trigger}}{\text{hie or c4 or eclmumu or lmlX}}, \tag{1}$$

and for an individual ECL trigger:

$$\epsilon = \frac{\text{(fff or ffo) and ECL trigger}}{\text{fff or ffo}}, \tag{2}$$

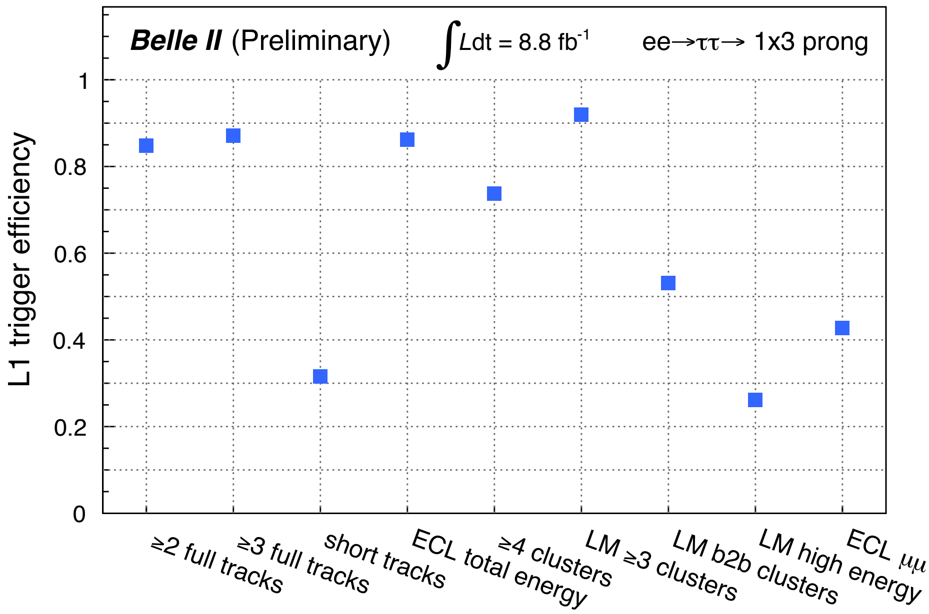

(a)

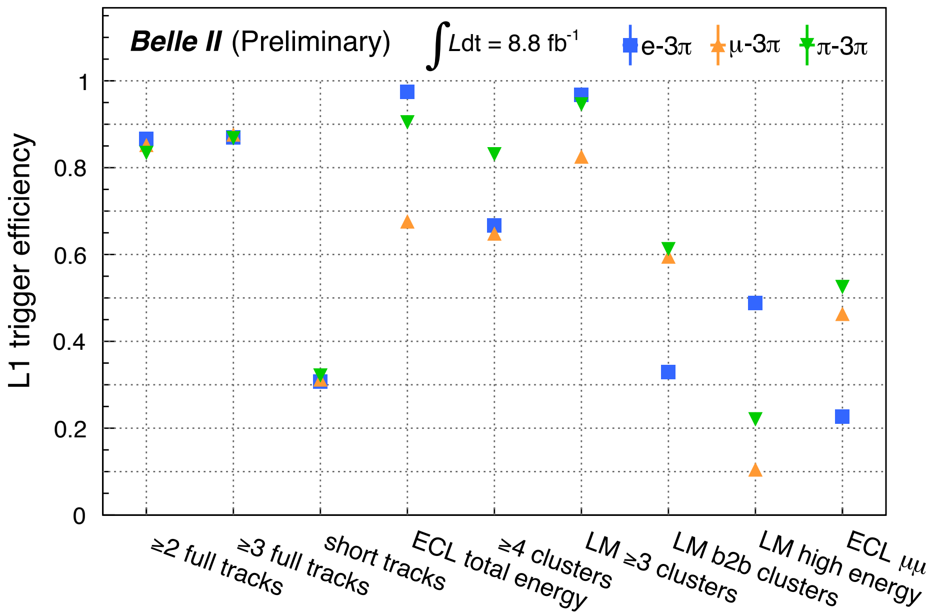

(b)

FIG. 1: The overall L1 trigger efficiencies for SM $ee \to \tau\tau \to 1{\times}3$ prong events in the (a) combined and (b) individual channels. The data comes from the 2019a, 2019b and 2019c periods. The following trigger combinations are considered: ≥ 2 full tracks (*ffo*), ≥ 3 full tracks (*fff*), short tracks (*fso* or *sso* or *ffs* or *fss* or *sss*), ECL total energy (*hie*), ≥ 4 clusters (*c4*), low multiplicity ≥ 3 clusters (*lml0* or *lml12*), low multiplicity back-to-back clusters (*lml8* or *lml9* or *lml10*), low multiplicity high energy cluster (*lml1* or *lml2* or *lml4* or *lml6* or *lml7*) and ECL $\mu\mu$ (*eclmumu*). Statistical uncertainties are shown, although they are too small to be visible.

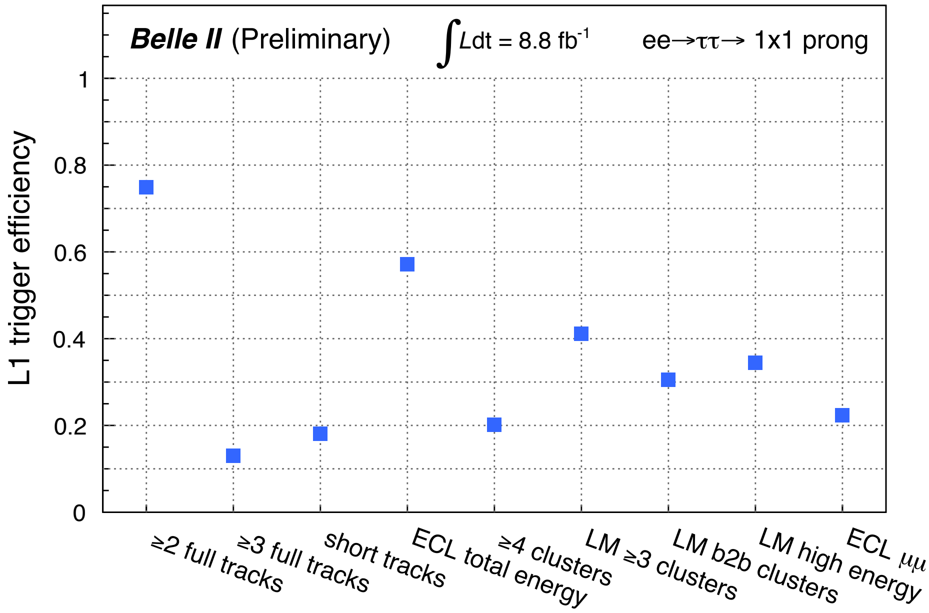

(a)

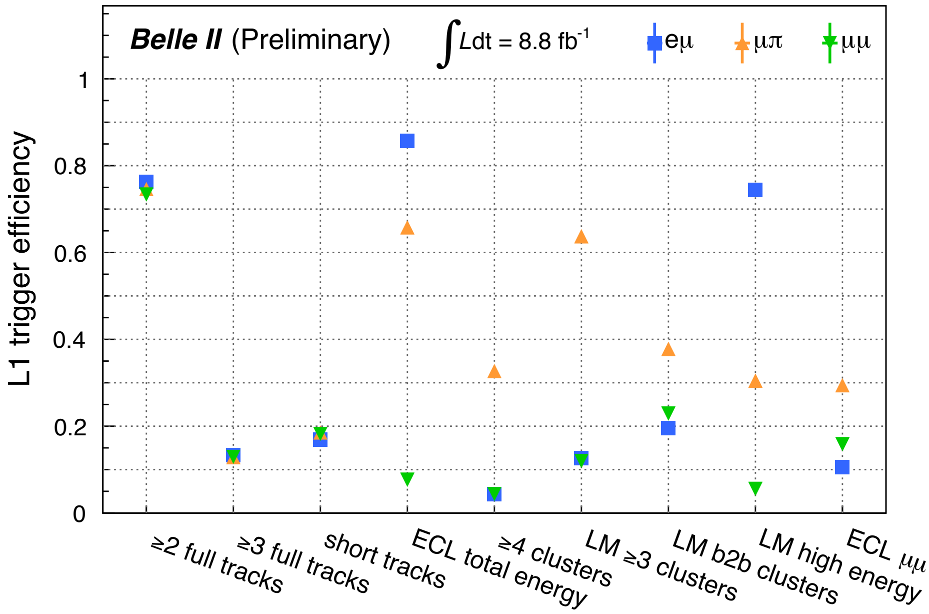

(b)

FIG. 2: The overall L1 trigger efficiencies for SM $ee \to \tau\tau \to 1{\times}1$ prong events in the (a) combined and (b) individual channels. The data comes from the 2019a, 2019b and 2019c periods. The following trigger combinations are considered: $\geq$ 2 full tracks (*ffo*), $\geq$ 3 full tracks (*fff*), short tracks (*fso* or *sso* or *ffs* or *fss* or *sss*), ECL total energy (*hie*), $\geq$ 4 clusters (*c4*), low multiplicity $\geq$ 3 clusters (*lml0* or *lml12*), low multiplicity back-to-back clusters (*lml8* or *lml9* or *lml10*), low multiplicity high energy cluster (*lml1* or *lml2* or *lml4* or *lml6* or *lml7*) and ECL $\mu\mu$ (*eclmumu*). Statistical uncertainties are shown, although they are too small to be visible.

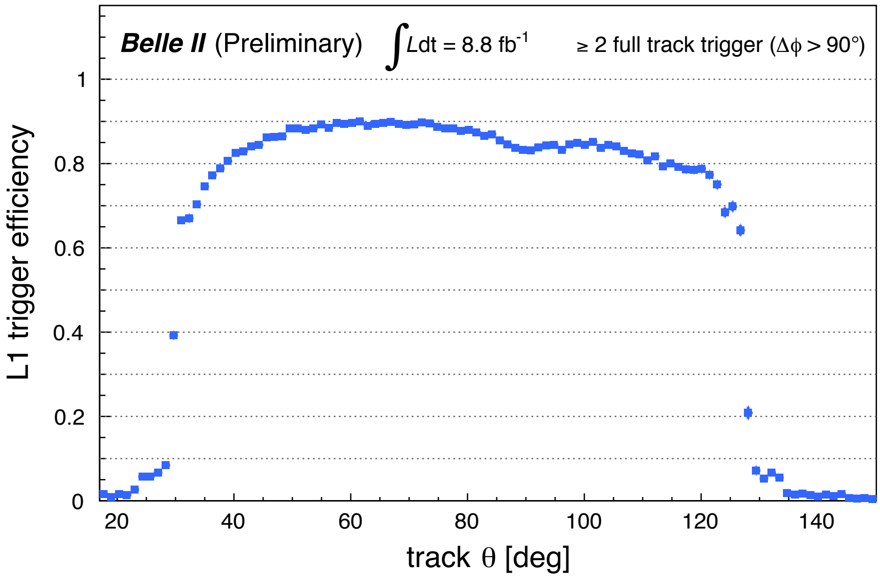

(a)

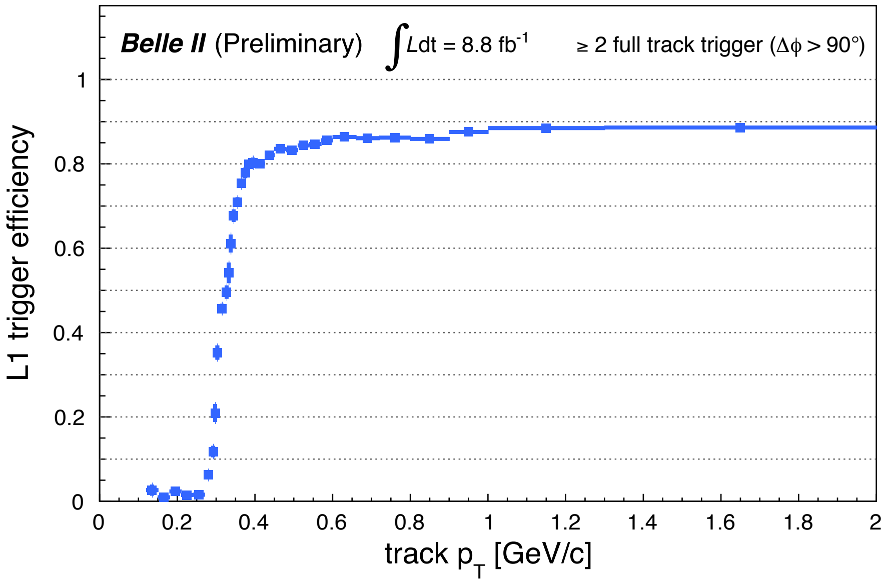

(b)

FIG. 3: The efficiency of the *ffo* trigger for SM $ee \to \tau\tau \to 1{\times}1$ prong events. This trigger requires at least two full tracks, a track pair with $\Delta\phi > 90^\circ$ and an ECL Bhabha veto at L1. The efficiency is shown as a function of the (a) θ and (b) p_T of the track with minimum p_T. The data sample was collected during the 2019a, 2019b and 2019c periods. Statistical uncertainties are shown.

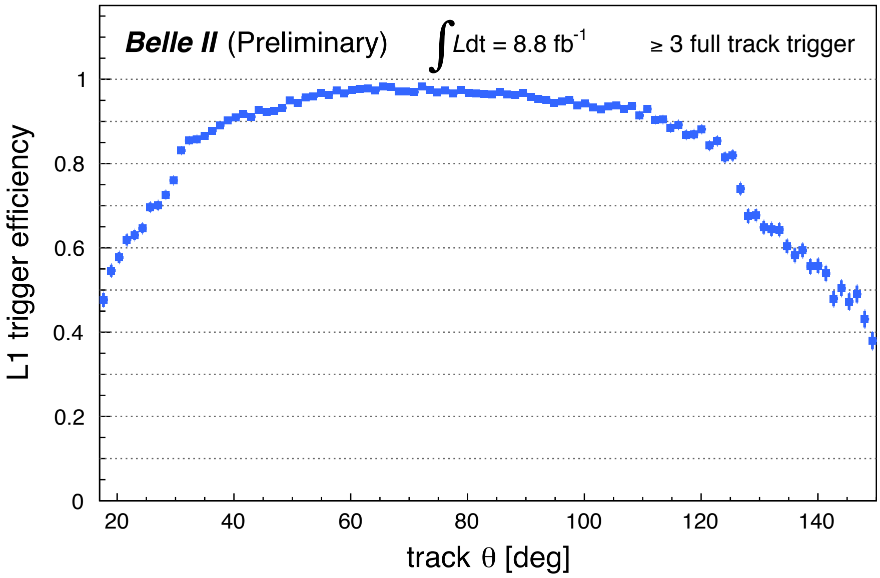

(a)

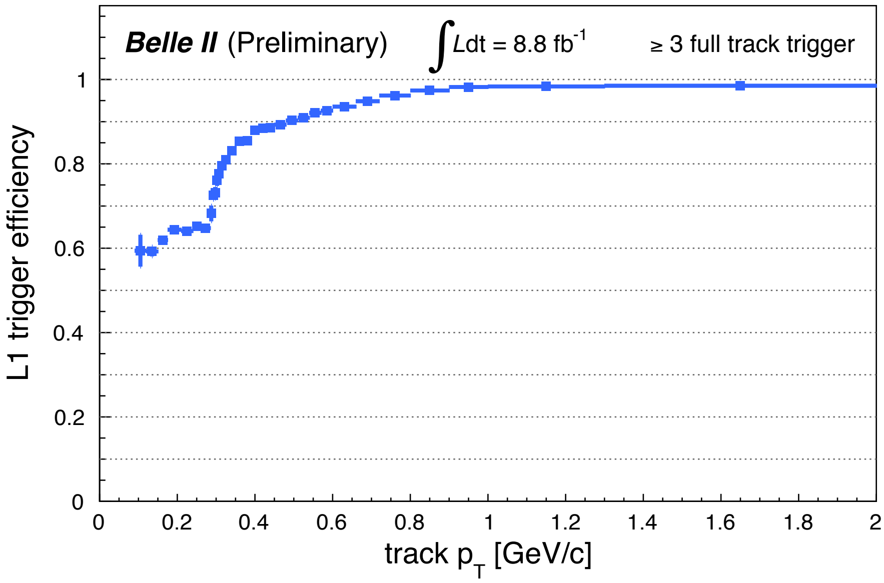

(b)

FIG. 4: The efficiency of the *fff* trigger for SM $ee \to \tau\tau \to 1{\times}3$ prong events. This trigger requires at least three full tracks at L1. The efficiency is shown as a function of the (a) θ and (b) p_T of the track with minimum p_T. The data sample was collected during the 2019a, 2019b and 2019c periods. Statistical uncertainties are shown.

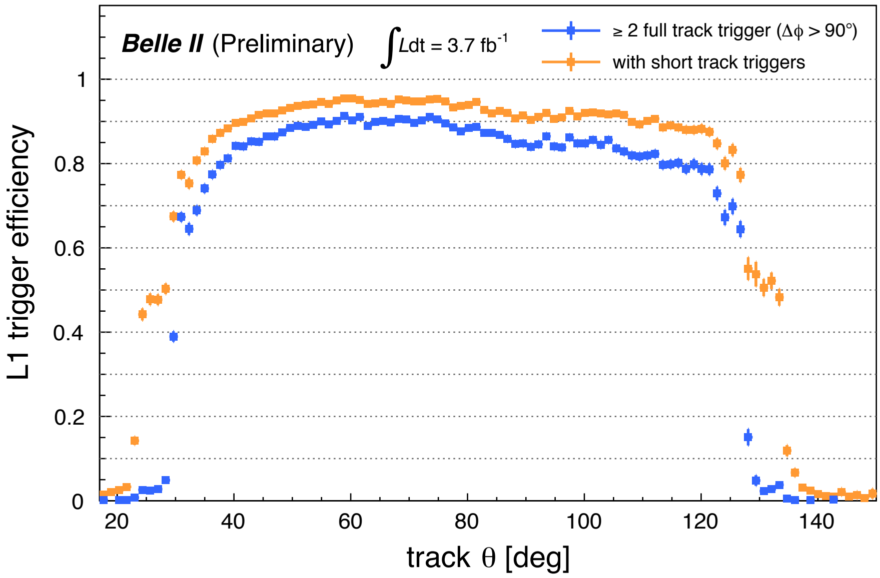

(a)

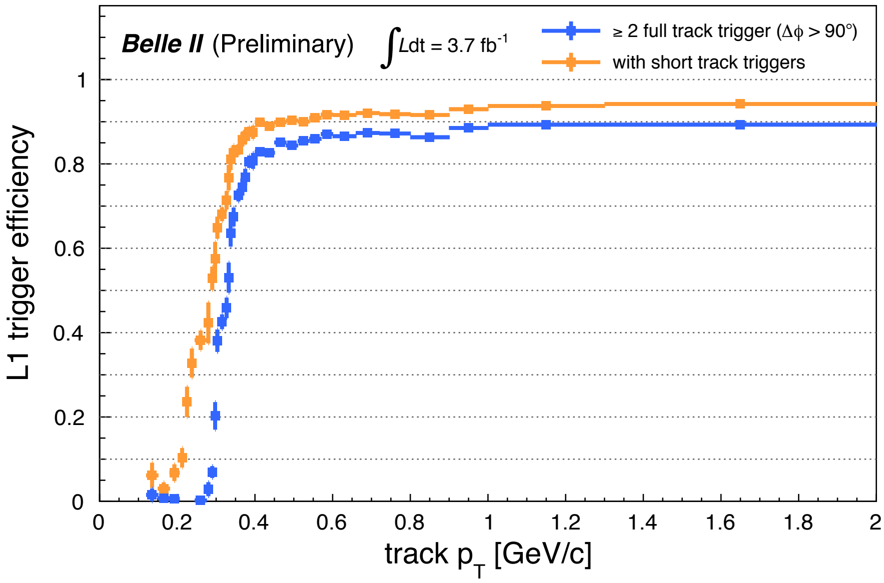

(b)

FIG. 5: The gain in efficiency when using the *ffo* trigger in conjunction with short track triggers (*ffo* or *fso* or *sso*) for SM $ee \to \tau\tau \to 1{\times}1$ prong events. The efficiency is shown as a function of the (a) θ and (b) p_T of the track with minimum p_T. The data sample was collected during the 2019c period. Statistical uncertainties are shown.

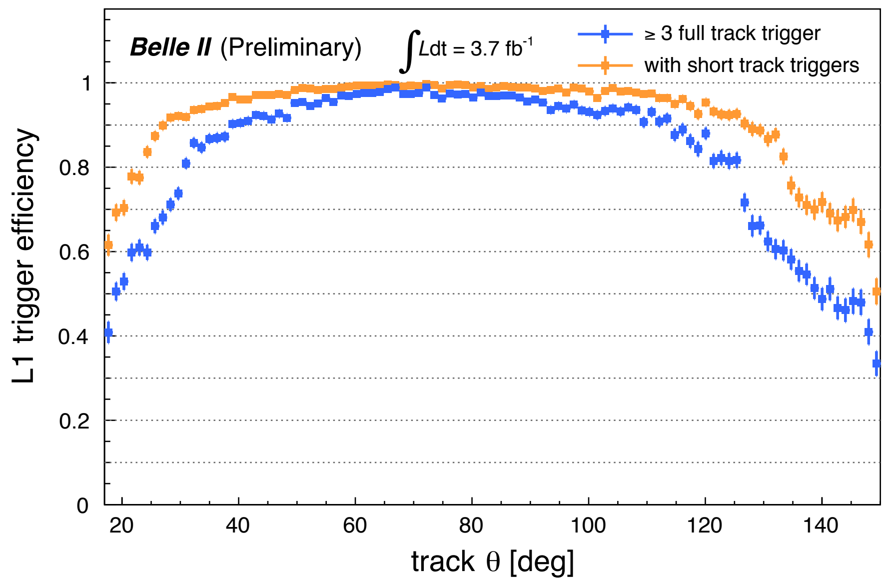

(a)

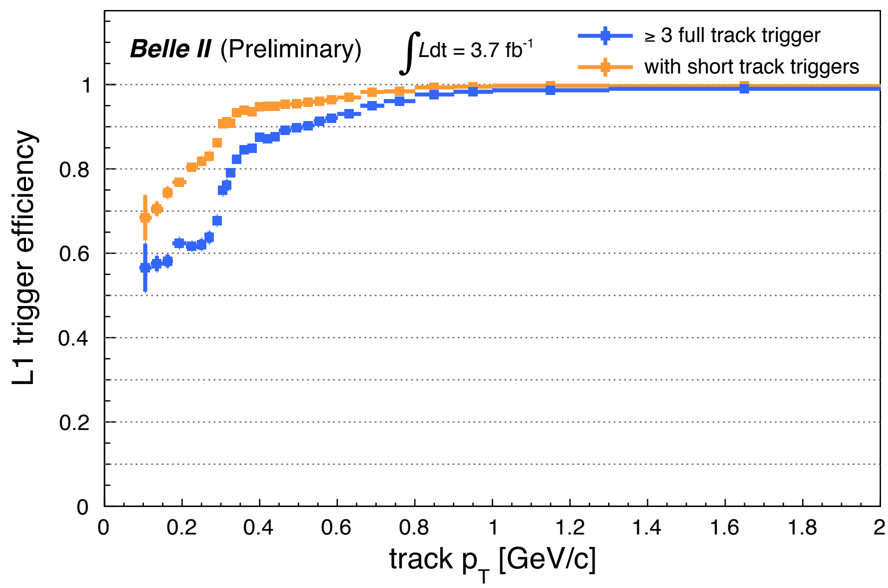

(b)

FIG. 6: The gain in efficiency when using the *fff* trigger in conjunction with short track triggers (*fff* or *ffs* or *fss* or *sss*) for SM $ee \to \tau\tau \to 1{\times}3$ prong events. The efficiency is shown as a function of the (a) θ and (b) p_T of the track with minimum p_T. The data sample was collected during the 2019c period. Statistical uncertainties are shown.

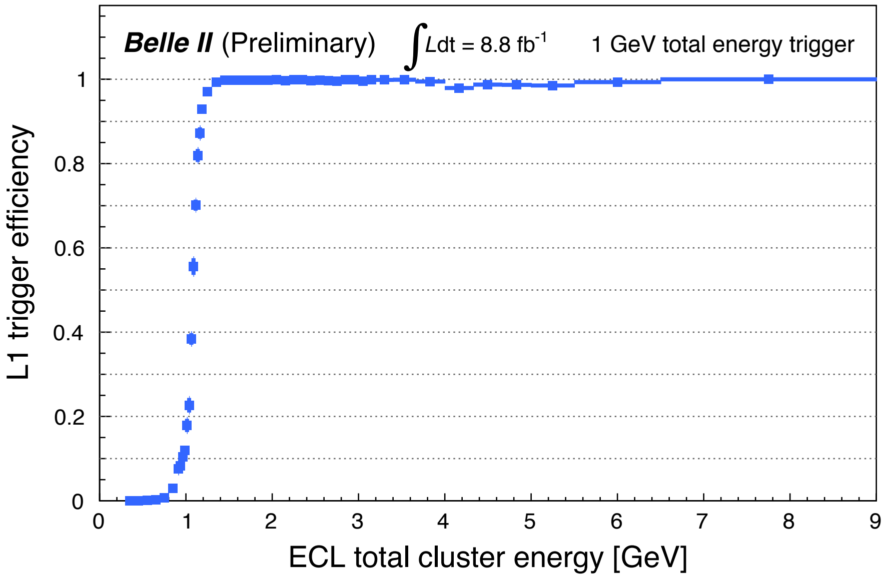

(a)

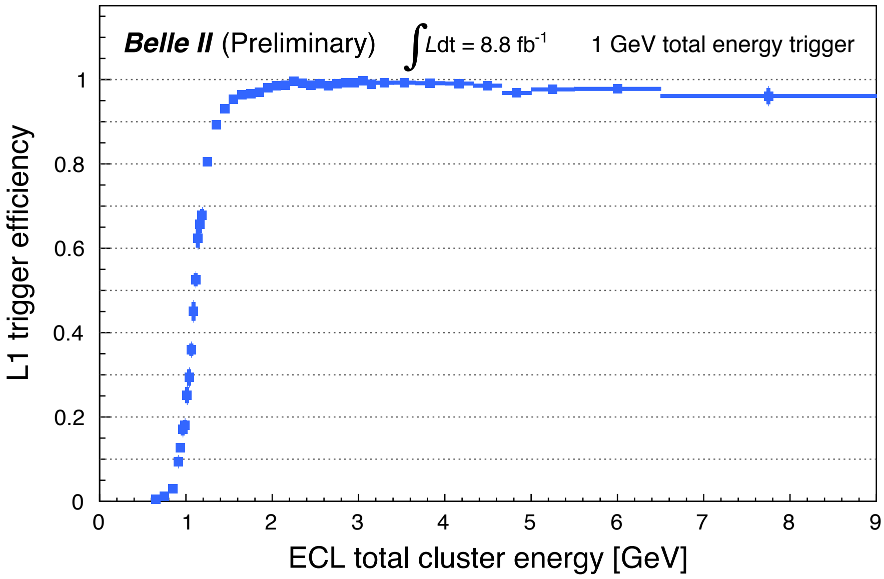

(b)

FIG. 7: The efficiency of the *hie* trigger as a function of the ECL total cluster energy for (a) SM $ee \to \tau\tau \to 1{\times}1$ prong and (b) $1{\times}3$ prong events. This trigger has a 1 GeV total energy threshold and Bhabha veto requirement at L1. The data sample was collected during the 2019a, 2019b and 2019c periods. Statistical uncertainties are shown.

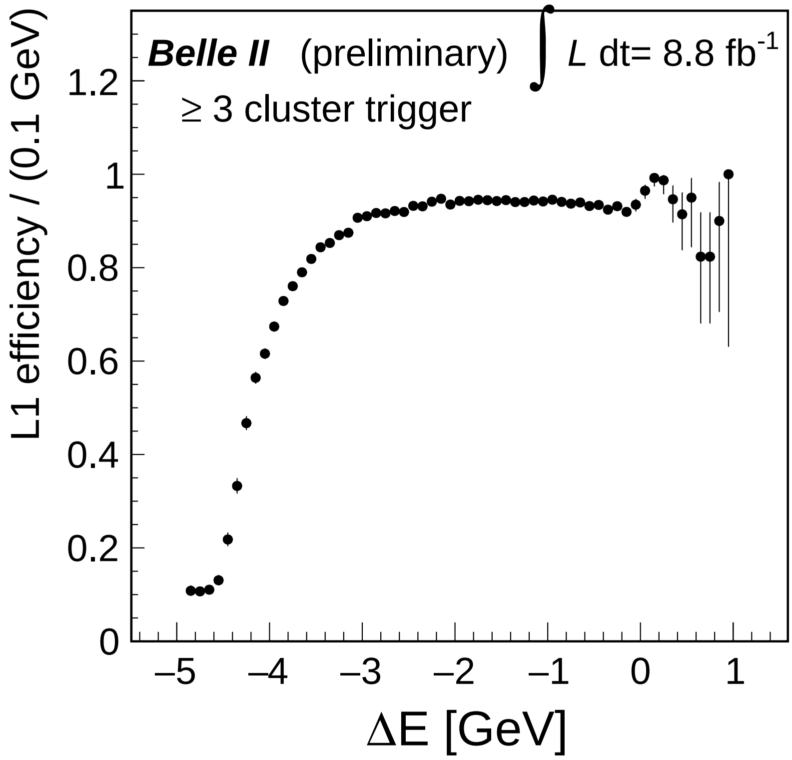

(b)

FIG. 8: The efficiency of the low multiplicity ≥ 3 cluster triggers (*lml0* or *lml12*) for τ LFV-like events as a function of the signal-side ΔE . SM 1×3 prong events are considered that mimic the kinematics of the $\tau \to 3\mu$ LFV process. The data sample was collected during the 2019a, 2019b and 2019c periods. Statistical uncertainties are shown.

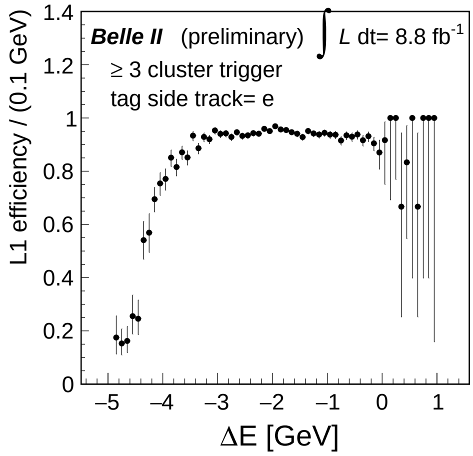

(a)

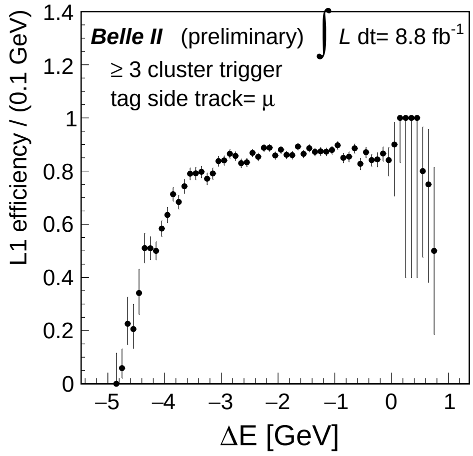

(b)

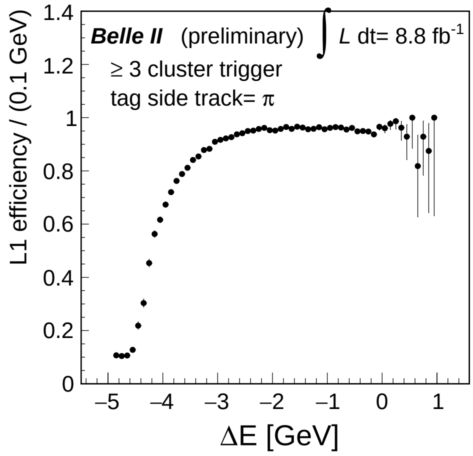

(c)

FIG. 9: The efficiency of the low multiplicity ≥ 3 cluster triggers (*lml0* or *lml12*) for τ LFV-like events as a function of the signal-side ΔE . SM $1{\times}3$ prong events are considered that mimic the kinematics of the $\tau \to 3\mu$ LFV process. The tag-side track is identified as an (a) electron, (b) muon or (c) charged pion. The data sample was collected during the 2019a, 2019b and 2019c periods. Statistical uncertainties are shown.